Available online at www.sciencedirect.com
ScienceDirect
International Journal of Thermal Sciences 46 (2007) 328–341
International Journal of Thermal Sciences
www.elsevier.com/locate/ijts

Mathematical modeling of continuous flow microwave heating of liquids (effects of dielectric properties and design parameters)

J. Zhu [a], A.V. Kuznetsov [a,*], K.P. Sandeep [b]

[a] *Department of Mechanical and Aerospace Engineering, North Carolina State University, Campus Box 7910, Raleigh, NC 27695-7910, USA*
[b] *Department of Food Science, North Carolina State University, Campus Box 7910, Raleigh, NC 27695-7624, USA*

Received 25 December 2005; accepted 20 June 2006

Available online 13 July 2006

Abstract

A detailed numerical model is presented to study heat transfer in liquids as they flow continuously in a circular duct that is subjected to microwave heating. Three types of food liquids are investigated: apple sauce, skim milk, and tomato sauce. The transient Maxwell's equations are solved by the finite difference time domain (FDTD) method to describe the electromagnetic field in the microwave cavity and the waveguide. The temperature field inside the applicator duct is determined by the solution of the momentum, energy, and Maxwell's equations. Simulations aid in understanding the effects of dielectric properties of the fluid, the applicator diameter and its location, as well as the geometry of the microwave cavity on the heating process. Numerical results show that the heating pattern strongly depends on the dielectric properties of the fluid in the duct and the geometry of the microwave heating system.

Keywords: Continuous microwave heating; Maxwell's equations; Non-Newtonian fluids

1. Introduction

Microwave heating is utilized to process materials for decades. In contrast to other conventional heating methods, microwave heating allows volumetric heating of materials. Without the need for any intermediate heat transfer medium, microwave radiation penetrates the material directly. Microwave energy causes volumetric heat generation in the material, which results in high energy efficiency and a reduction in heating time.

A distinct drawback to microwave heating is the lack of uniformity in material heating [1–3]. Both the magnitude and spatial distribution of microwave energy are dictated by the complexity of electromagnetic waves scattering and reflecting in the microwave unit, as well as absorption of electromagnetic waves within the material [4]. Factors that influence microwave heating include dielectric properties, volume, and shape of the material, as well as design and geometric parameters of the microwave unit [5]. These factors make it difficult to precisely control the heating process in order to obtain the desired temperature distribution in the material. Due to complexity of the physical process, numerical modeling has been widely utilized to study microwave heating [6].

In the past, a number of studies [7–14] have been documented that dealt with numerical modeling of microwave heating process in a cavity. Generally, prediction of microwave energy deposition requires the solution of Maxwell's equations, which determines the electromagnetic field in the microwave cavity and waveguide. The finite difference time domain (FDTD) method developed by Yee [15] has been widely utilized to solve Maxwell's equations. Solutions of Maxwell's equations using the FDTD method for a number of simplified cases are reported in Webb et al. [16]. Three-dimensional simulations of microwave propagation and energy deposition are presented in Liu et al. [9], Zhao and Turner [17], and Zhang et al. [18].

Success in the numerical simulation of electromagnetic propagation has recently generated interest in numerical modeling of heat transfer induced by microwave radiation. Clemens and Saltiel [4] developed a model of microwave heating of a solid specimen. Their model accounts for temperature depen-

* Corresponding author.
E-mail address: avkuznet@eos.ncsu.edu (A.V. Kuznetsov).

1290-0729/$ – see front matter
doi:10.1016/j.ijthermalsci.2006.06.005

Nomenclature

A	area	m^2	
C_p	specific heat capacity	$J\,kg^{-1}\,K^{-1}$	
c	phase velocity of the electromagnetic propagation wave	$m\,s^{-1}$	
E	electric field intensity	$V\,m^{-1}$	
f	frequency of the incident wave	Hz	
h	effective heat transfer coefficient	$W\,m^{-2}\,K^{-1}$	
H	magnetic field intensity	$A\,m^{-1}$	
L	standard deviation of temperature	°C	
k	thermal conductivity	$W\,m^{-1}\,K^{-1}$	
m	fluid consistency coefficient	$Pa\,s^n$	
n	flow behavior index		
N	number of time steps		
p	pressure	Pa	
q	electromagnetic heat generation intensity	$W\,m^{-3}$	
Q	microwave power absorption	W	
T	temperature	°C	
t	time	s	
$\tan\delta$	loss tangent		
$\mathbf{v}$	fluid velocity vector	$m\,s^{-1}$	
w	velocity component in the z direction	$m\,s^{-1}$	
W	width of the incident plane	m	
Z_{TE}	wave impedance	Ω	

Greek symbols

η	apparent viscosity	Pa s
ε	electric permittivity	$F\,m^{-1}$
ε'	dielectric constant	
ε''	effective loss factor	
ε_{rad}	emissivity	
λ_g	electromagnetic wavelength in the cavity	m
μ	magnetic permeability	$H\,m^{-1}$
ρ	density	$kg\,m^{-3}$
σ	electric conductivity	$S\,m^{-1}$
σ_{rad}	Stefan–Boltzmann constant	$W\,m^{-2}\,K^{-4}$

Superscripts

τ	instantaneous value

Subscripts

∞	ambient condition
0	free space, air
t	time
in	input
X, Y, Z	projection on a respective coordinate axis

dent dielectric properties, which causes coupling between the Maxwell's and energy equations. Effects of the microwave frequency, dielectric properties of the specimen, and the size of the sample on the microwave energy deposition were investigated in a two-dimensional formulation. Other important papers addressing modeling of microwave heating processes include Ayappa et al. [19–21], Basak and Ayappa [22], and Ratanadecho et al. [23,24].

Although most previous studies of microwave heating focused on conduction heat transfer in a specimen, a few recent papers investigated natural convection induced by microwave heating of liquids; mathematical models utilized in these papers included the momentum equation. Datta et al. [25] investigated natural convection in a liquid subjected to microwave heating. In their study, the microwave energy deposition was assumed to decay exponentially into the sample based on Lambert's law, which is valid only for a high loss dielectric material and a sample of large size. Therefore, for small size samples or low loss dielectric materials, coupled Maxwell's, momentum, and energy equations must be solved.

Ratanadecho et al. [26] were the first who investigated, numerically and experimentally, microwave heating of a liquid layer in a rectangular waveguide. The movement of liquid particles induced by microwave heating was taken into account. Coupled electromagnetic, hydrodynamic and thermal fields were simulated in two dimensions. The spatial variation of the electromagnetic field was obtained by solving Maxwell's equations with the FDTD method. Their work demonstrated the effects of microwave power level and liquid electric conductivity on the degree of penetration and the rate of heat generation within the liquid layer. Furthermore, an algorithm for resolving the coupling of Maxwell's, momentum, and energy equations was developed and validated by comparing with experimental results.

Microwave heating of a liquid flowing in a rectangular duct passing through a cubic cavity was studied in [27]. Temperature distributions in different liquids were simulated. The aim of this research is to investigate heating of a liquid in a geometry which better approximates that of real industrial systems. The geometry is similar to that investigated in [28,29], but extended to three dimensions. Numerical simulations of microwave heating of a liquid continuously flowing in a circular pipe are reported. Velocity distribution is assumed to be that of a fully developed non-Newtonian flow in a circular pipe. If more microwave energy is released in the center of the pipe and less is released near the wall, the outlet temperature distribution may be closer to uniform. In this paper, a microwave cavity designed to generate exactly such energy distribution is investigated. An algorithm similar to that reported in [26] is utilized in this study to couple Maxwell's and energy equations. In order to optimize the design of the microwave system, the effects of the diameter of the applicator tube, the location of the applicator tube in the microwave cavity, and the shape of the microwave cavity are investigated.

2. Model geometry

Fig. 1 shows the schematic diagram of the microwave system examined in this research. The system consists of a waveguide, a resonant cavity, and a vertically positioned applicator tube that

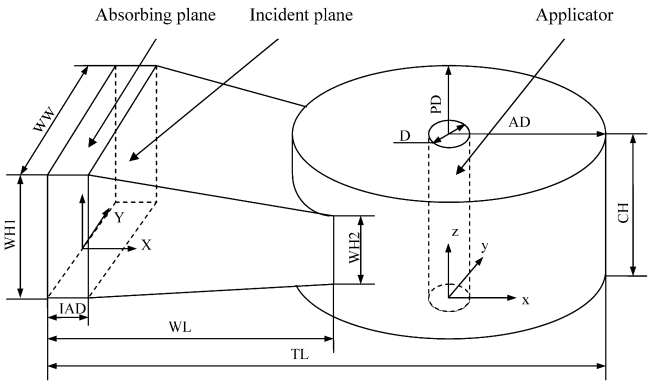

Fig. 1. Schematic diagram of the problem.

Table 1
Geometrical parameters

Symbol	Description	Value [mm]
D	Applicator diameter	30.4–55.7
AD	Apogee distance of cavity	128–205
PD	Perigee distance of cavity	154
CH	Cavity & applicator height	125
WL	Waveguide length	347
WW	Waveguide width	244
WH1	Waveguide height	125
WH2	Waveguide height	51
TL	Total length of the system	661
IAD	Distance between the incident plane and absorbing plane	27

passes through the cavity. A liquid food, which is treated as a non-Newtonian fluid, flows through the applicator tube in the upward direction, absorbing the microwave energy as it passes through the tube. It is assumed that no phase change occurs during the heating process. The microwave operates in TE_{10} [30] mode at a frequency of 915 MHz; the microwave energy is generated at the incident plane by imposing a plane polarized source. The microwave is transmitted through the waveguide towards the applicator tube located in the center of the resonant cavity. An absorbing plane is placed behind the incident plane to absorb the microwave energy reflected from the cavity. Two computational domains are utilized. The first domain, used for electromagnetic computations, includes the region enclosed by the wall of the waveguide, resonant cavity, and incident plane. The second domain, used for solving the momentum and energy equations, coincides with the region inside the applicator tube. The origin of the coordinate system for the electromagnetic computational domain lies at a corner of the waveguide, as shown in Fig. 1. The origin of the coordinate system for the inside of the applicator tube is in the center of the tube at the tube entrance. Parameters characterizing system's geometry are listed in Table 1.

3. Mathematical model formulation

3.1. Electromagnetic field

Maxwell's equations governing the electromagnetic field are expressed in terms of the electric field, **E**, and the magnetic field, **H**. In the Cartesian coordinate system, (X, Y, Z), they are presented as:

$$\frac{\partial H_X}{\partial t} = \frac{1}{\mu}\left(\frac{\partial E_Y}{\partial Z} - \frac{\partial E_Z}{\partial Y}\right) \tag{1}$$

$$\frac{\partial H_Y}{\partial t} = \frac{1}{\mu}\left(\frac{\partial E_Z}{\partial X} - \frac{\partial E_X}{\partial Z}\right) \tag{2}$$

$$\frac{\partial H_Z}{\partial t} = \frac{1}{\mu}\left(\frac{\partial E_X}{\partial Y} - \frac{\partial E_Y}{\partial X}\right) \tag{3}$$

$$\frac{\partial E_X}{\partial t} = \frac{1}{\varepsilon}\left(\frac{\partial H_Z}{\partial Y} - \frac{\partial H_Y}{\partial Z} - \sigma E_X\right) \tag{4}$$

$$\frac{\partial E_Y}{\partial t} = \frac{1}{\varepsilon}\left(\frac{\partial H_X}{\partial Z} - \frac{\partial H_Z}{\partial X} - \sigma E_Y\right) \tag{5}$$

$$\frac{\partial E_Z}{\partial t} = \frac{1}{\varepsilon}\left(\frac{\partial H_Y}{\partial X} - \frac{\partial H_X}{\partial Y} - \sigma E_Z\right) \tag{6}$$

where σ is the electric conductivity, μ is the magnetic permeability, and ε is the electric permittivity. Subscripts X, Y, and Z denote respective components of the vectors **E** and **H**.

Boundary and initial conditions for the electromagnetic fields are:

(a) At the walls of the waveguide and cavity, a perfect conducting condition is utilized. Therefore, normal components of the magnetic field and tangential components of the electric field vanish at these walls:

$$H_n = 0, \qquad E_t = 0 \tag{7}$$

(b) At the absorbing plane, Mur's first order absorbing condition [31] is utilized:

$$\left(\frac{\partial}{\partial Z} - \frac{1}{c}\frac{\partial}{\partial t}\right) E_Z\big|_{X=0} = 0 \tag{8}$$

where c is the phase velocity of the propagation wave.

(c) At the incident plane, the input microwave source is simulated by the equations:

$$E_{Z,inc} = -E_{Zin}\sin\left(\frac{\pi Y}{W}\right)\cos\left[2\pi\left(ft - \frac{X_{in}}{\lambda_g}\right)\right] \tag{9}$$

$$H_{Y,inc} = \frac{E_{Zin}}{Z_{TE}}\sin\left(\frac{\pi Y}{W}\right)\cos\left[2\pi\left(ft - \frac{X_{in}}{\lambda_g}\right)\right] \tag{10}$$

where f is the frequency of the microwave, W is the width of the incident plane, Z_{TE} is the wave impedance, λ_g is the wave length of a microwave in the waveguide, and E_{Zin} is the input value of the electric field intensity. By applying the Poynting theorem [26], the input value of the electric field intensity is evaluated by the microwave power input as:

$$E_{Zin} = \sqrt{\frac{4Z_{TE}P_{in}}{A}} \tag{11}$$

where P_{in} is the microwave power input and A is the area of the incident plane.

(d) The applicator wall is assumed to be electromagnetically transparent.

(e) At $t = 0$ all components of **E** and **H** are zero.

3.2. Energy and momentum equations

The temperature distribution in the applicator tube is obtained by the solution of the following energy equation with a source term which accounts for internal energy generation due to the absorption of the microwave energy:

$$\rho C_p\left(\frac{\partial T}{\partial t}+w\frac{\partial T}{\partial z}\right)=\nabla\cdot(k\nabla T)+q(x,y,z,t) \tag{12}$$

where ρ is the density; C_p is the specific heat; k is the thermal conductivity; T is the temperature; w is the axial velocity of the fluid; t is the time; and x, y, and z are the Cartesian coordinates. q represents the local electromagnetic heat generation intensity term, which depends on dielectric properties of the liquid and the electric field intensity:

$$q=2\pi f\varepsilon_0\varepsilon'(\tan\delta)E^2 \tag{13}$$

In Eq. (13), ε_0 is the permittivity of the air; ε' is the dielectric constant of the liquid; and $\tan\delta$ is the loss tangent, a dimensionless parameter defined as:

$$\tan\delta=\frac{\varepsilon''}{\varepsilon'} \tag{14}$$

where ε'' stands for the effective loss factor. The dielectric constant, ε', characterizes the penetration of the microwave energy into the product, while the effective loss factor, ε'', indicates the ability of the product to convert the microwave energy into heat [32]. Both ε' and ε'' are dependent on the microwave frequency and the temperature of the product. $\tan\delta$ indicates the ability of the product to absorb microwave energy.

The velocity of the fluid flow is determined by the solution of the following continuity and momentum equations:

$$\nabla\cdot\mathbf{v}=0 \tag{15}$$

$$\rho\frac{D\mathbf{v}}{Dt}=-\nabla p+\nabla\cdot\eta\nabla\mathbf{v} \tag{16}$$

where $\mathbf{v}$ is the velocity vector; p is the pressure; and η is the apparent viscosity of the non-Newtonian fluid, which in this study is assumed to obey the power-law [33], as:

$$\eta=m(\dot\gamma)^{n-1} \tag{17}$$

where m and n are the fluid consistency coefficient and the flow behavior index, respectively.

In this study, it is assumed that the flow is hydrodynamically fully developed; only the axial velocity component is non-zero. The momentum equation is then simplified as:

$$\frac{\partial}{\partial x}\left(\eta\frac{\partial w}{\partial x}\right)+\frac{\partial}{\partial y}\left(\eta\frac{\partial w}{\partial y}\right)-\frac{\mathrm{d}p}{\mathrm{d}z}=0 \tag{18}$$

The apparent viscosity, η, is expressed as:

$$\eta=m\left[\left(\frac{\partial w}{\partial x}\right)^2+\left(\frac{\partial w}{\partial y}\right)^2\right]^{(n-1)/2} \tag{19}$$

The following boundary conditions are utilized to determine the velocity and temperature distributions. At the inner surface of the applicator tube, a hydrodynamic no-slip boundary condition is used. At the inlet to the applicator, a uniform, fully developed velocity profile is imposed, and specified by the inlet mean velocity, V_{mean}.

Table 2
Thermophysical and electromagnetic parameters utilized in computations

f, MHz		915
P_{in}, W		5000
μ, H m^{-1}		$4\pi\times10^{-7}$
ε_0, F m^{-1}		8.854×10^{-12}
T_∞, °C		20
V_{mean}, m s^{-1}		0.03
h, W m^{-2} K^{-1}		15
ε_{rad}		0.4
Z_{TE}, Ω		377
k, W m^{-1} K^{-1}	Apple sauce	0.5350
	Skim milk	0.5678
	Tomato sauce	0.5774
c_p, J kg^{-1} K^{-1}	Apple sauce	3703.3
	Skim milk	3943.7
	Tomato sauce	4000.0
ρ, kg m^{-3}	Apple sauce	1104.9
	Skim milk	1047.7
	Tomato sauce	1036.9
m	Apple sauce	32.734
	Skim milk	0.0059
	Tomato sauce	3.9124
n	Apple sauce	0.197
	Skim milk	0.98
	Tomato sauce	0.097

The following thermal boundary condition is imposed at the applicator wall. The wall is assumed to lose heat by natural convection and radiation:

$$-k\left.\frac{\partial T}{\partial n}\right|_{surface}=h(T-T_\infty)+\sigma_{rad}\varepsilon_{rad}\left(T^4-T_\infty^4\right) \tag{20}$$

where T_∞ is the ambient air temperature (the waveguide walls are assumed to be in thermal equilibrium with the ambient air), σ_{rad} is the Stefan–Boltzmann constant, ε_{rad} is the surface emissivity of the wall of the applicator tube, n is the normal direction to the surface of the wall, and h is the effective heat transfer coefficient defined as:

$$h=\frac{1}{1/h_{air}+L_{wall}/k_{wall}+1/h_{liquid}} \tag{21}$$

In Eq. (21), h_{air} is the heat transfer coefficient between the applicator wall and the air in the cavity, h_{liquid} is the heat transfer coefficient between the liquid inside the applicator and the wall, L_{wall} is the thickness of the applicator wall, and k_{wall} is the thermal conductivity of the wall. The inlet liquid temperature is assumed to be uniform and equal to the temperature in the free space outside the applicator, T_∞. The initial temperature of the liquid is defined as:

$$T=T_\infty \quad \text{at } t=0 \tag{22}$$

Table 2 lists thermophysical properties of the liquids considered in this study and other pertinent system parameters.

4. Numerical solution procedure

Maxwell's equations (1)–(6) are solved utilizing the FDTD method [34] on a uniform rectangular grid consisting of 2 472 000 cells in the electromagnetic computational domain. A leapfrog scheme [34] is applied to Maxwell's equations so that the components of the electric field intensity vector are one half cell offset in the direction of their corresponding components, while the magnetic field intensity components are one half cell offset in each direction orthogonal to their corresponding components [4]. The electric and magnetic fields are evaluated at alternate half time steps. The time step, Δt, must satisfy the Courant stability condition [34]:

$$\Delta t \leqslant \frac{1}{c\sqrt{\frac{1}{\Delta X^2}+\frac{1}{\Delta Y^2}+\frac{1}{\Delta Z^2}}} \tag{23}$$

In this research, a time step of $\Delta t = 1.56 \times 10^{-12}$ s is used to solve Maxwell's equations. Since a portion of the boundary of the resonant cavity surface is curved, a staircase grid is utilized to approximate this curved surface. The grid size is $\mathrm{d}X = \mathrm{d}Y = 1.28$ mm and $\mathrm{d}Z = 6.25$ mm. A contour-path integral FDTD method [35] is utilized to deal with the curved surface of the microwave cavity using traditional rectangular cells.

Energy and momentum equations (12) and (18) are discretized using a cell centered finite volume approach and are solved implicitly in the Cartesian coordinate system using the time step of 0.1 s. An upwind scheme is adopted to represent advection in the thermal fluid flow domain. To approximate a cylindrically shaped applicator tube, a staircase grid with rectangular cells is utilized.

Since in Eq. (13) the dielectric constant, ε', and the loss tangent, $\tan\delta$, are temperature dependent, an iterative scheme is required to resolve the coupling between the energy and Maxwell's equations. Since the time scale for electromagnetic transients (a nanosecond scale) is much smaller than that for the flow and thermal transport (0.1 s), the electromagnetic heat source, q, defined by Eq. (13), is computed in terms of the time average field, $\overline{E}$, which is treated as a constant over one time step for the thermal-flow computation, and defined as:

$$\overline{E} = \frac{1}{N}\sum_{\tau=1}^{N} E^{\tau} \tag{24}$$

where N is the number of time steps in each period of the microwave and E^{τ} is the instantaneous electric field intensity. The details of the numerical scheme used in this study are given in [4]. Energy equation (13) is solved by an implicit scheme, at each time step iterations are continued until the following convergence criterion is met:

$$\left|\frac{T^{k+1}_{i,j,k,t} - T^{k}_{i,j,k,t}}{T^{k}_{i,j,k,t}}\right| \leqslant 10^{-6} \tag{25}$$

where the superscript k refers to the kth iteration. Since this study is focused on steady-state temperature profiles, iterative computations of electromagnetic and thermal fields continue until the temperature distribution does not change with time.

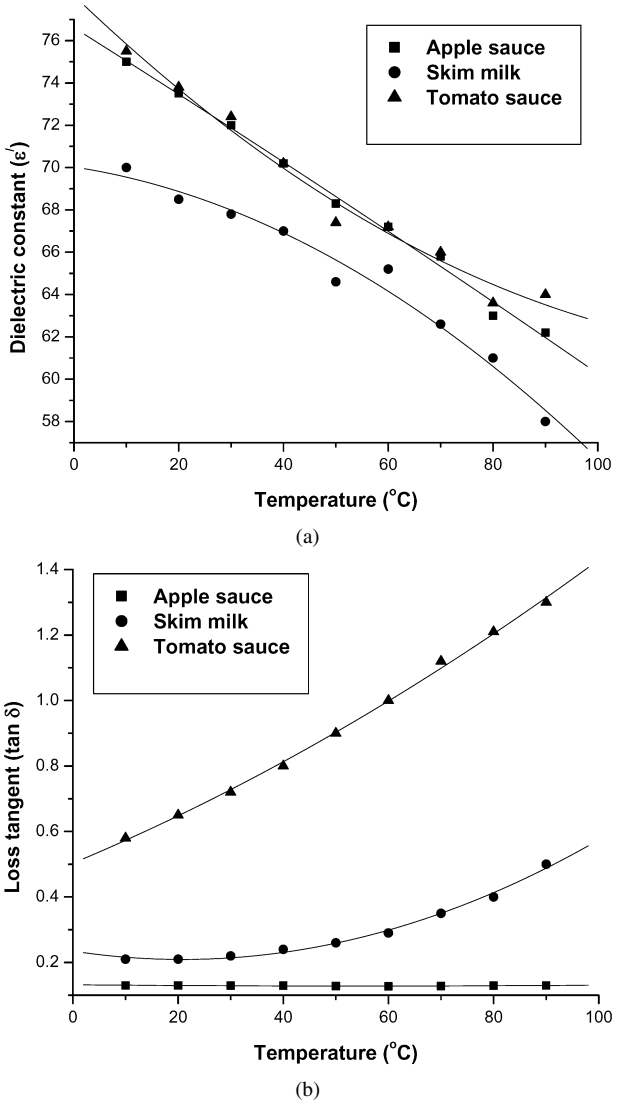

Fig. 2. Temperature dependent dielectric properties: (a) dielectric constant, ε'; (b) loss tangent, $\tan\delta$.

The convergence criterion is defined as $\Delta = |\frac{T^{t+1}_{i,j,k} - T^{t}_{i,j,k}}{T^{t}_{i,j,k}}|$ and convergence to steady-state, similarly to Eq. (25), is declared when $\Delta \leqslant 10^{-6}$.

5. Results and discussion

In this study, three liquid food products are considered, specifically, apple sauce, skim milk, and tomato sauce. The temperature-dependent data for the dielectric constant and loss tangent for the three liquids are plotted versus temperature in Fig. 2. In order to compare the results obtained for variant system geometries, the base case is first defined. The base case is characterized by the following geometric parameters of the microwave system: the applicator diameter is 38 mm, it is placed in the center of the resonant cavity, and the apogee distance of the resonant cavity is 154 mm. Presented results correspond to the moment in time when the temperature attains its steady-state. It takes about 1100 time steps for the temperature to reach

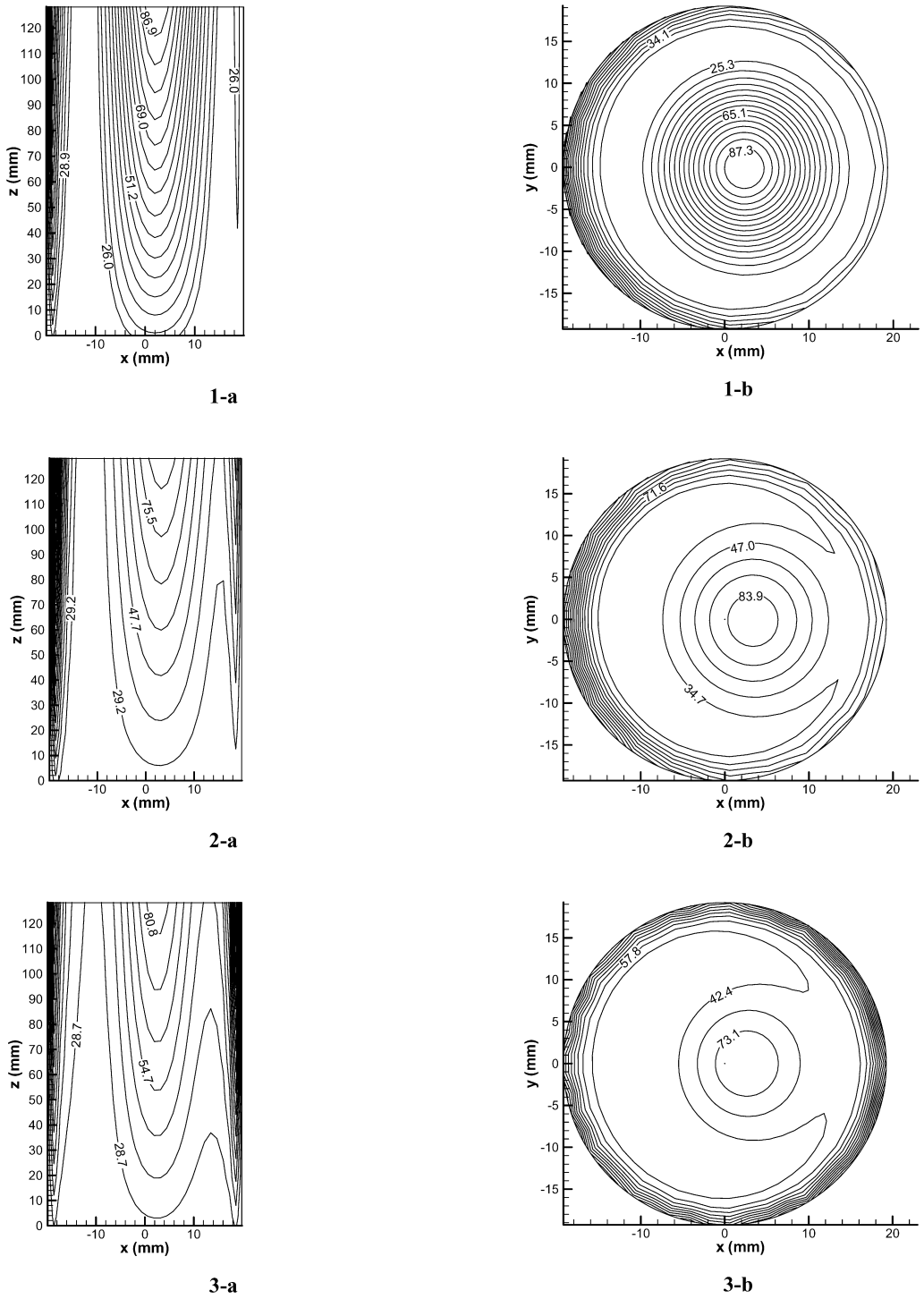

Fig. 3. Temperature distributions [°C] in (a) x–z plane ($y = 0$), and (b) x–y plane (outlet, $z = 124$ mm) for apple sauce (1), skim milk (2), and tomato sauce (3), respectively.

its steady-state. The corresponding CPU time is about 50 hours on a single 208 Intel Xeon 3.0 GHz processor.

5.1. Heating patterns for liquids with different dielectric properties

The spatial distribution of the temperature and the corresponding electromagnetic power intensity for the three liquids are presented in Figs. 3 and 4. Results are shown in the vertical x–z plane ($y = 0$) and the horizontal x–y plane at the applicator outlet ($z = 124$ mm), respectively. The system geometry corresponding to the base case is investigated. The evidence of interaction of the electromagnetic field and forced convection in the three liquids is seen in Fig. 3. As the fluid particle enters the applicator tube, it is heated by the microwave radiation. As the temperature increases in the z-direction, dielectric properties

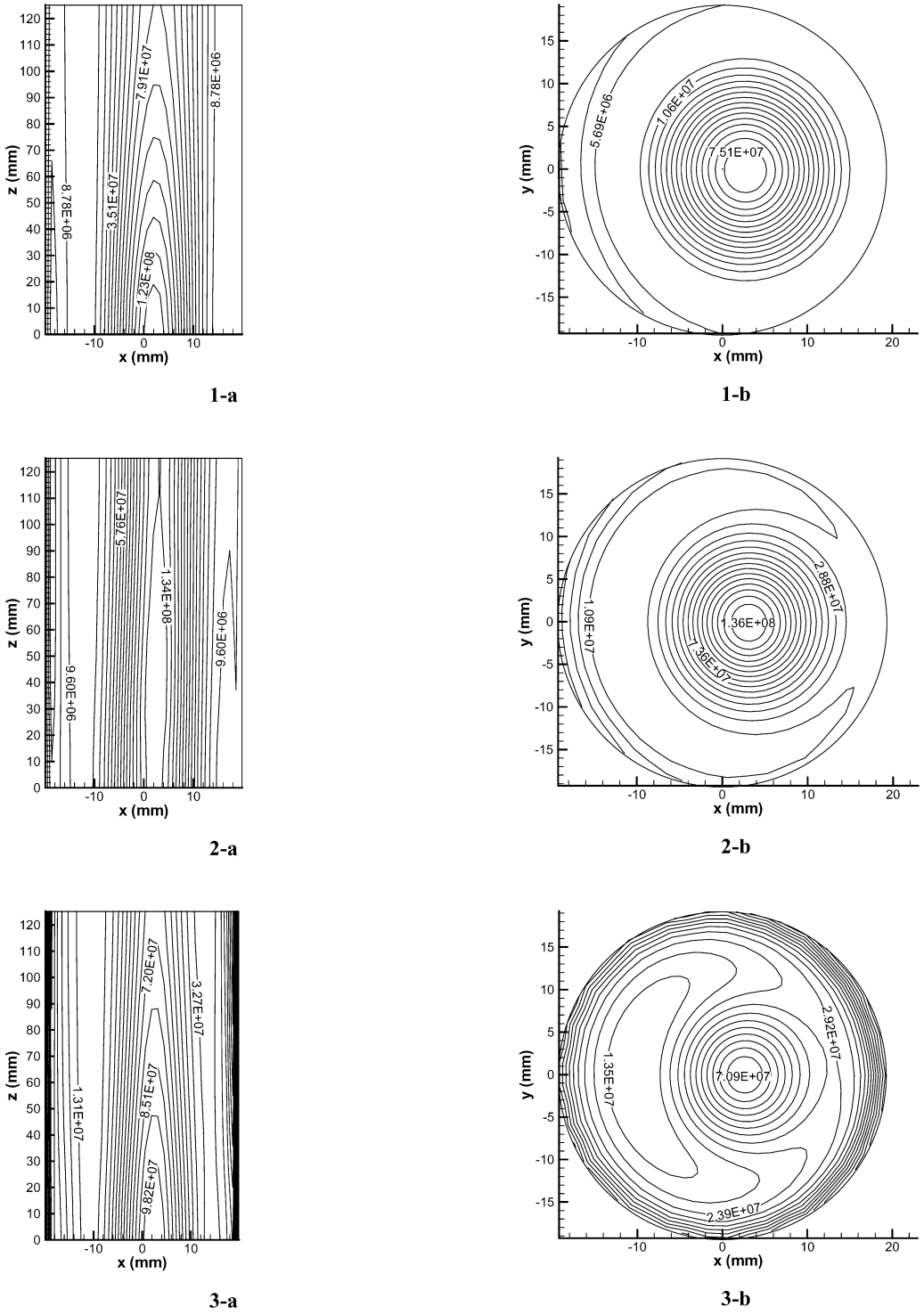

Fig. 4. Electromagnetic power intensity distributions [W m^{-3}] in (a) x–z plane ($y = 0$), and (b) x–y plane (outlet, $z = 124$ mm) for apple sauce (1), skim milk (2), and tomato sauce (3), respectively.

of the liquid change in accordance with Fig. 2, which changes the distribution of electromagnetic field in the microwave cavity and the distribution of electromagnetic power intensity in the applicator. However, since the dielectric properties of the liquids considered in this study are not highly temperature dependent, the electromagnetic power intensity does not change greatly in the z-direction, as shown in Fig. 4.

It is evident that the electromagnetic power determines the temperature distribution in the x–y plane. As expected, Fig. 4 shows a well-defined peak of electromagnetic power intensity near the center of the applicator tube; the peak is shifted by approximately 3 mm in the x-direction for all three liquids. Although most of the microwave energy is released near the center of the tube, the reduced velocity near the wall results

Table 3
Dimensionless power absorption in different liquids

Liquids	Dielectric constant, ε' (50 °C)	Loss tangent, $\tan\delta$ (50 °C)	Dimensionless power absorption
Apple sauce	68.4	0.12	0.613
Skim milk	64.6	0.31	0.889
Tomato sauce	69.3	0.92	0.998

in higher temperature in the region near the wall for all three liquids. Comparing the power density and temperature distributions for apple sauce and skim milk, it is evident that the peak value of the power density near the tube center for apple sauce is approximately half as large as that for skim milk, but the temperature of the corresponding hot spot occurring in apple sauce is larger. This is because the flow behavior index, n, for apple sauce ($n = 0.197$) is much smaller than that for skim milk ($n = 0.98$), so that the velocity profile for skim milk is sharper and the magnitude of the velocity in the core region is larger. The high velocity in the core region reduces the effect of the peak of the electromagnetic power intensity on the temperature of the corresponding hot spot in skim milk.

To illustrate the effect of dielectric properties on power absorption, Table 3 shows the dimensionless total electromagnetic power (non-dimensionalized by the input power) absorbed by three liquids, defined as:

$$\widetilde{Q} = \frac{Q_{total}}{P_{in}} \tag{26}$$

The total power absorbed, Q_{total}, can be calculated by integrating the electromagnetic heat generation intensity over the domain occupied by the applicator tube:

$$Q_{total} = \iiint_V q \,\mathrm{d}x\,\mathrm{d}y\,\mathrm{d}z \tag{27}$$

The results confirm that a lower loss tangent liquid absorbs less microwave power as compared to a higher loss tangent liquid. The relation between the loss tangent and the microwave power absorption can be expressed by the reflection coefficient, R. For a normal incidence of the electromagnetic wave on a plane boundary between the material and vacuum, the reflection coefficient (the fraction of reflected power), R, is [36]:

$$R = \frac{1 - \sqrt{2\varepsilon'[1+\sqrt{1+(\tan\delta)^2}]} + \varepsilon'\sqrt{1+(\tan\delta)^2}}{1 + \sqrt{2\varepsilon'[1+\sqrt{1+(\tan\delta)^2}]} + \varepsilon'\sqrt{1+(\tan\delta)^2}} \tag{28}$$

Apparently, for the same dielectric constant, larger loss tangent and smaller reflection coefficient correspond to larger power absorption. From Table 3, it is evident that 99.8% of the electromagnetic power is absorbed by tomato sauce, 88.9% by skim milk, and 61.3% by apple sauce. The remainder of the electromagnetic power is reflected and absorbed by the absorbing plane.

Table 4
Dimensionless power absorption: effect of the applicator diameter

Liquids	Applicator diameter, D [mm]						
	30.4	35.5	38	40.5	45.6	50.7	55.7
Apple sauce	0.518	0.519	0.613	0.725	0.768	0.483	0.343
Skim milk	0.830	0.870	0.889	0.952	0.973	0.771	0.572
Tomato sauce	0.948	0.991	0.998	0.975	0.873	0.736	0.630

Table 5
Mean temperature increase at the outlet: effect of the applicator diameter

Liquids	Applicator diameter, D [mm]						
	30.4	35.5	38	40.5	45.6	50.7	55.7
Apple sauce	1.35	0.846	0.926	1.026	1.072	0.560	0.302
Skim milk	2.687	1.572	1.688	1.805	1.861	1.373	0.770
Tomato sauce	2.638	2.213	2.152	1.858	1.313	0.947	0.682

5.2. Effect of the applicator diameter

Tables 4 and 5 show the dimensionless electromagnetic power absorption and the mean temperature increase at the outlet, which is non-dimensionalized by the inlet temperature as:

$$\Delta\widetilde{T} = \frac{\overline{T} - T_\infty}{T_\infty} \tag{29}$$

where $\overline{T}$ is the mean temperature at the outlet of the applicator. The diameters of the applicator tubes are chosen to be 30.4, 35.5, 38, 40.5, 45.6, 50.7, and 55.7 mm, respectively. The effect of the diameter is investigated for the geometry of the microwave cavity corresponding to the base case. The inlet mean velocity is the same for all cases ($V_{mean} = 0.03\ \mathrm{m\,s^{-1}}$). From Table 4, it is evident that in tomato sauce the power absorption increases as the diameter of the applicator is increased from 30.4 to 38 mm. This is because increasing the diameter enlarges the effective surface area for microwave penetration into the liquid. However, as the applicator diameter is further increased from 40.5 to 55.7 mm, the power absorption decreases. This phenomenon is explained using the concept of the cut-off frequency, which is defined as:

$$f_c = \frac{c}{2}\lambda \tag{30}$$

Microwaves cannot propagate into the waveguide when the frequency is below the cut-off frequency because they cannot propagate between guiding surfaces separated by less than one half of the wavelength. Therefore, the effective surface area for microwave penetration into the liquid is reduced (microwaves cannot get to a part of the applicator surface which is too close to the walls of the resonant cavity) and the energy generation in the liquid decreases accordingly [4]. In this case, $\frac{\lambda}{2} = 164$ mm, which is even larger than the perigee distance of the microwave cavity. However, since the liquid in the applicator is not a perfectly conducting material and a portion of the microwave energy can therefore penetrate through the applicator, the cut-off distance is actually smaller than 164 mm in this case. Comparing the power absorption in apple sauce, skim milk, and tomato sauce, it is evident that the critical diameter, which is defined as the diameter of the applicator above which the microwave

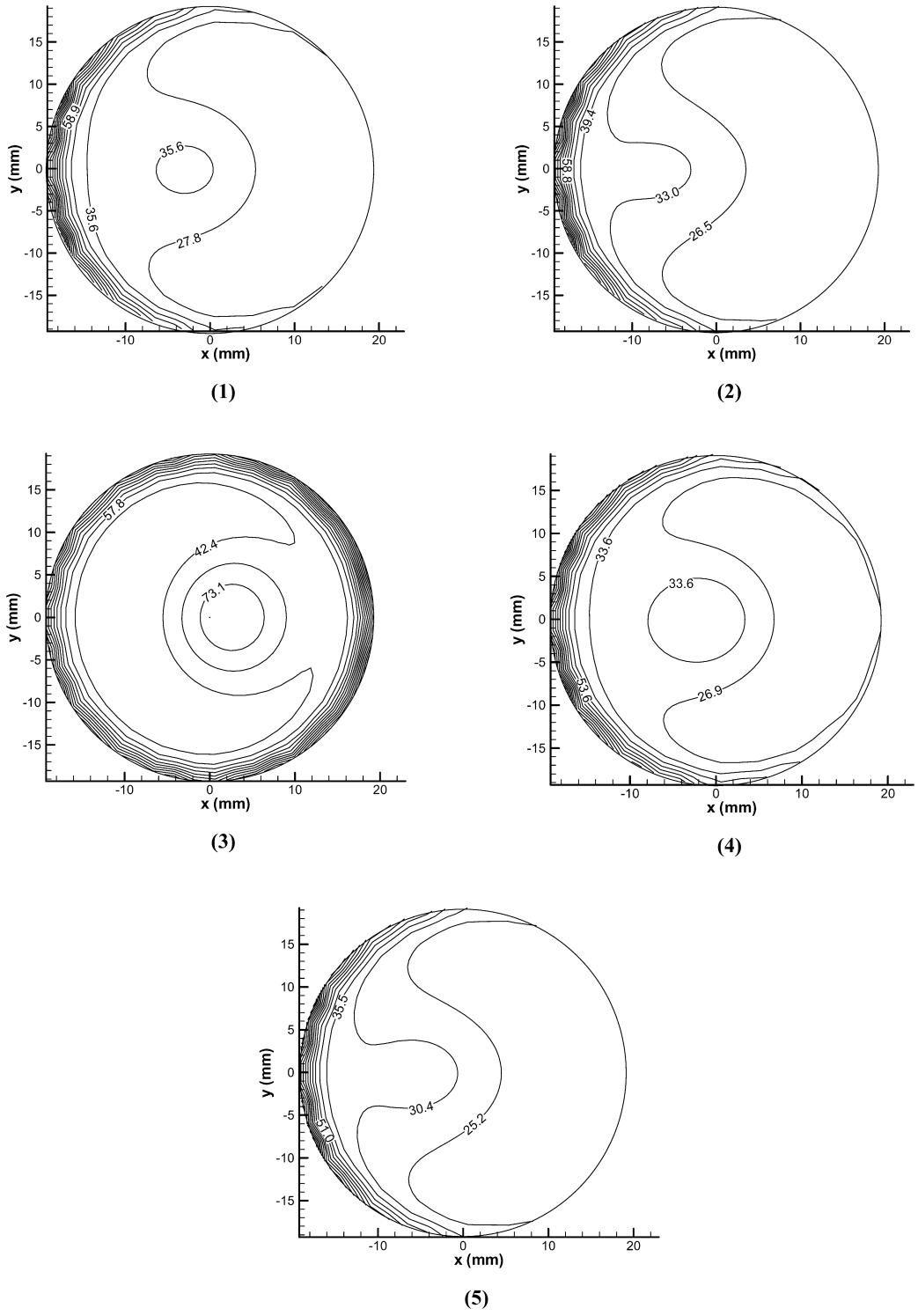

Fig. 5. Temperature distributions [°C] for tomato sauce at the outlet ($z = 124$ mm): effect of the applicator position; the applicator is shifted in the x-direction from its position in the base case by (1) −136 mm, (2) −68 mm, (2) 0 mm, (4) +68 mm, (5) +136 mm, respectively.

power absorption decreases with the increase of the applicator diameter, is different for the three liquids. For apple sauce and skim milk it is approximately 45.6 mm, but for tomato sauce it is approximately 38 mm. This is attributed to the effect of fluid dielectric properties. Since in tomato sauce the power absorption starts decreasing with the diameter increase at a smaller applicator diameter than in skim milk, for applicator diameters of 40.5 and 45.6 mm the power absorption in skim milk is larger than that in tomato sauce, although tomato sauce has a higher loss tangent.

From Table 5, it is evident that the mean temperature increase at the outlet does not necessarily exhibit the same trend as the power absorption. For example, in apple sauce, although the power absorption increases when the diameter

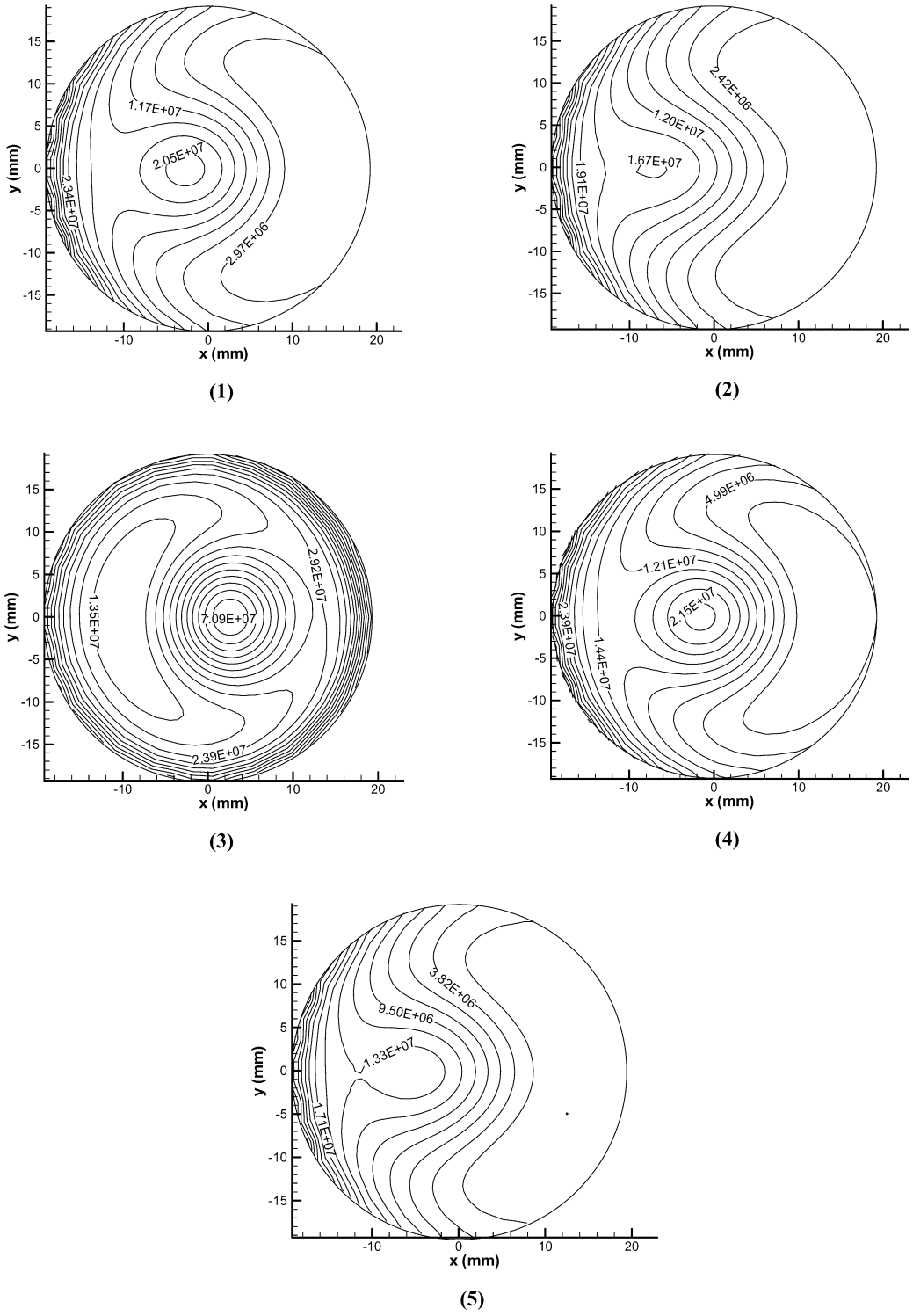

Fig. 6. Electromagnetic power intensity distributions [W m^{-3}] for tomato sauce at the outlet ($z = 124$ mm): effect of the applicator position; the applicator is shifted in the x-direction from its position in the base case by (1) −136 mm, (2) −68 mm, (2) 0 mm, (4) +68 mm, (5) +136 mm, respectively.

is increased from 30.4 to 35.5 mm, the corresponding mean temperature increase becomes smaller. Recalling that the inlet mean flow velocity is the same for all applicator diameters, the mass flow rate is smaller for the applicator with a smaller diameter. Since the increase of the power absorption in the applicator with a diameter of 35.5 mm is not significant, which is explained by a higher resonance in the cavity with the 30.4 mm diameter applicator, the temperature increase in the applicator with a smaller diameter (30.4 mm) is larger. Thus in order to obtain the maximum temperature increase, one should select the applicator with the diameter of 30.4 mm.

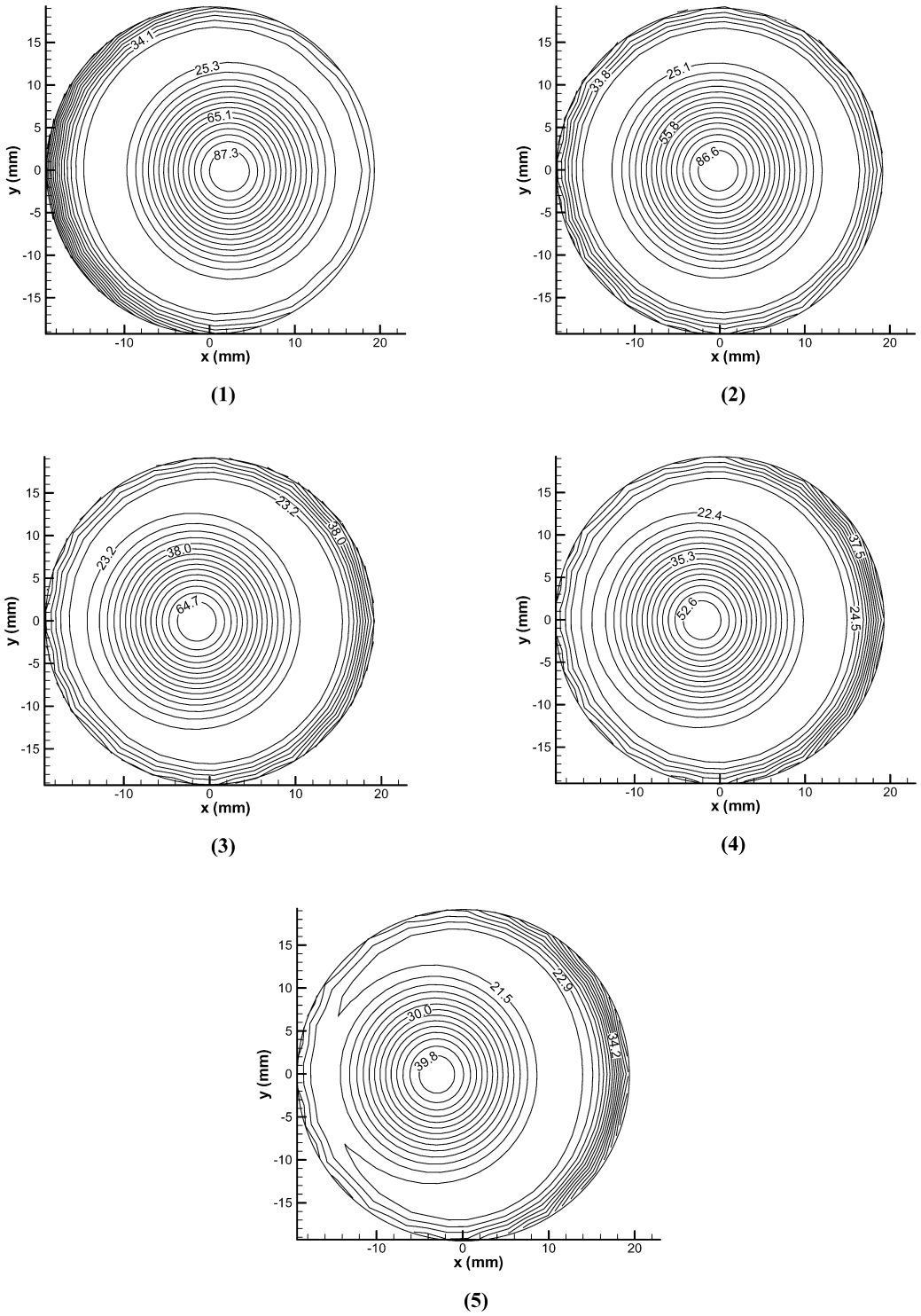

Fig. 7. Temperature distributions [°C] for apple sauce at the outlet ($z = 124$ mm): effect of the resonant cavity shape; (1) apogee distance of 205 mm, (2) 186 mm, (3) 167 mm, (4) 154 mm, and (5) 128 mm, respectively.

5.3. Effect of different locations of the applicator on the heating process

This section discusses the effect of positioning the applicator at different locations in the microwave cavity. Five different locations of the applicator are investigated. The geometry with the applicator positioned in the center of the microwave cavity is treated as the base case, other four cases correspond to -136, -68, $+68$, and $+136$ mm shifts in the x-direction, respectively, from the position of the applicator in the base case. The diameter of the applicator is 38 mm for all five applicator positions. Figs. 5 and 6 show the temperature and electromagnetic power intensity distributions in tomato sauce at the outlet ($z = 124$ mm) for the applicator positioned at five dif-

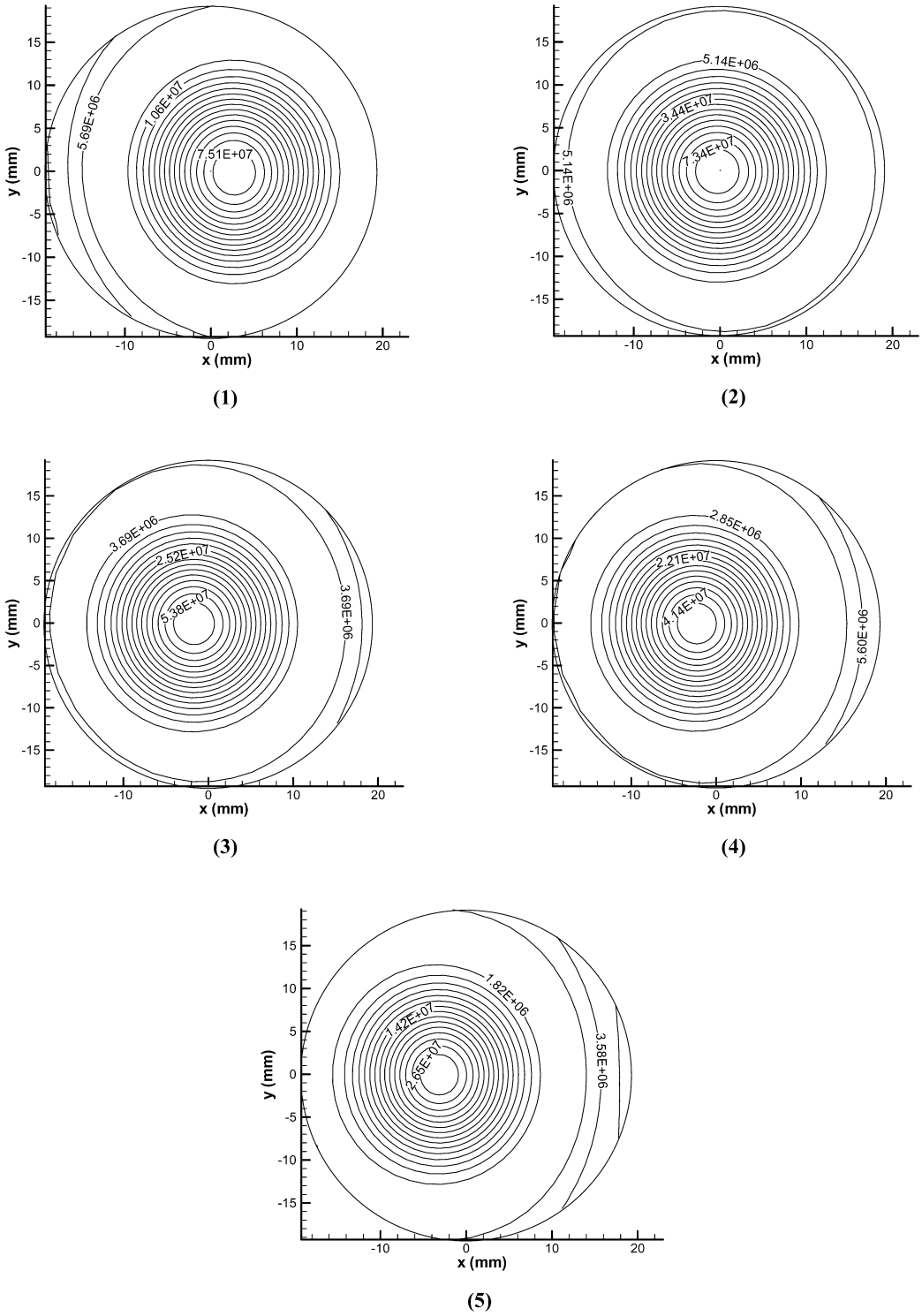

Fig. 8. Electromagnetic power intensity distributions [W m^{-3}] for apple sauce at the outlet ($z = 124$ mm): effect of the resonant cavity shape; (1) apogee distance of 205 mm, (2) 186 mm, (3) 167 mm, (4) 154 mm, and (5) 128 mm, respectively.

ferent locations in the microwave cavity. It is evident that the temperature and microwave power intensity decreases significantly if the applicator is shifted from the base case position. This is because the cross section of the resonant cavity is ellipsoidal, and the guiding distance of the resonant cavity is the largest for the plane corresponding to $x = 0$. The guiding distance is decreased by moving the applicator either forward or backward, reducing the effective surface area of the applicator available for the microwave penetration due to reduced distance between the applicator and the wall of the cavity to the extent that microwaves are not able to get to a portion of the applicator surface. In Fig. 6, unlike the base case, most of the microwave energy is absorbed in the front ($x < 0$) half of the applicator, implying that microwaves are strongly attenuated as they prop-

Table 6
Dimensionless power absorption: effect of the applicator location

Liquids	Location of applicator				
	−136 mm shift in x	−68 mm shift in x	Base case (no shift)	+68 mm shift in x	+136 mm shift in x
Apple sauce	0.141	0.110	0.613	0.140	0.093
Skim milk	0.233	0.193	0.889	0.226	0.159
Tomato sauce	0.284	0.233	0.998	0.290	0.196

agate around the applicator and the effective surface area for the microwave penetration is reduced to the front half part of the applicator surface. The heat energy generation decreases as well. Table 6 shows the effect of positioning of the applicator on electromagnetic power absorption in apple sauce, skim milk and tomato sauce. It is evident that for all three liquids the power absorption is the greatest when the applicator is in the base case position. The power absorption is greatly attenuated by shifting the applicator away from the base case position. Positioning the applicator in the center of the cavity thus provides the maximum heating rate.

5.4. Effect of the shape of the cavity

The effect of the shape of the resonant cavity is investigated. The height and the perigee distance of the resonant cavity are kept unchanged. The shape of the cross section of the cavity is controlled by the apogee distance which is chosen to be 205, 186, 167, 154, and 128 mm, respectively. An applicator diameter of 38 mm is utilized. Figs. 7 and 8 show the outlet ($z = 124$ mm) temperature and electromagnetic power intensity distributions in apple sauce for different shapes of the cavity. From Fig. 8 it is evident that the peak of the electromagnetic power intensity moves backward (in the negative x-direction) and the magnitude of the power intensity decreases with reduced apogee distance. The decreasing trend of the power intensity can be attributed to the fact that the space of the cavity is reduced by decreasing the apogee distance, which reduces the resonance of the microwaves in the cavity. The effect of the cross section shape on the electromagnetic power absorption of apple sauce, skim milk, and tomato sauce is shown in Table 7. It is evident that the maximum heating rate can be achieved by utilizing the microwave cavity with the apogee distance of 205 mm. However, if the goal is to obtain the most uniform temperature distribution at the outlet cross-section, the apogee distance of 186 mm should be used. For this apogee distance, the maximum power absorption occurs in the area located most closely to the applicator axis. In this case the maximum power absorption is compensated by the smallest residence time of the liquid (because of the largest fluid velocity in the applicator center).

Table 7
Dimensionless power absorption: effect of the cavity shape

Liquids	Apogee distance, AD [mm]				
	205	186	167	154	128
Apple sauce	0.613	0.597	0.390	0.282	0.172
Skim milk	0.889	0.784	0.533	0.404	0.267
Tomato sauce	0.998	0.822	0.578	0.459	0.325

6. Conclusions

A numerical model is developed for simulating forced convection of a liquid continuously flowing in a circular applicator that is subjected to microwave heating. The results reveal a complicated interaction between electromagnetic field and convection. The effects of dielectric properties of the liquid, the diameter of the applicator tube, the location of the applicator tube in the cavity, and the shape of the cavity on heating patterns are investigated. Dielectric properties of the liquid determine the ability of the liquid to absorb the microwave energy; the geometry of the microwave system also plays an important role in the power absorption and distribution. Enlarging the diameter of the applicator increases the effective surface available to absorb the microwave energy, usually increases the power absorption in the liquid. However, beyond the critical diameter of the applicator, an opposite trend is observed. The critical diameter of the applicator depends on the geometry of the resonant cavity and dielectric properties of the liquid flowing in the applicator. The microwave power absorption is also sensitive to the location of the applicator and the shape of the resonant cavity, which affect the microwave propagation and resonance.

Acknowledgements

The authors acknowledge with gratitude a USDA grant that provided support for this work and the assistance of the Food Rheology Laboratory at North Carolina State University. The calibrations of the fluid consistency coefficients and the flow behavior indexes for the non-Newtonian liquids considered in this study by Ms. S. Ramsey are greatly appreciated.

References

[1] K.G. Ayappa, H.T. Davis, E.A. Davis, J. Gordon, Analysis of microwave heating of materials with temperature-dependent properties, AIChE Journal 37 (1991) 313–322.
[2] M. De Pourcq, Field and power density calculation in closed microwave system by three-dimensional finite difference, IEEE Proceedings 132 (1985) 361–368.
[3] X. Jia, P. Jolly, Simulation of microwave field and power distribution in a cavity by a three dimensional finite element method, Journal of Microwave Power and Electromagnetic Energy 27 (1992) 11–22.
[4] J. Clemens, C. Saltiel, Numerical modeling of materials processing microwave furnaces, International Journal of Heat and Mass Transfer 39 (1995) 1665–1675.

[5] R.C. Anantheswaran, L. Liu, Effect of viscosity and salt concentration on microwave heating of model non-Newtonian liquid foods in a cylindrical container, Journal of Microwave Power and Electromagnetic Energy 29 (1994) 119–126.
[6] Q. Zhang, T.H. Jackson, A. Ungan, Numerical modeling of microwave induced natural convection, International Journal of Heat and Mass Transfer 43 (2000) 2141–2154.
[7] X. Jia, M. Bialkowski, Simulation of microwave field and power distribution in a cavity by a three dimensional finite element method, Journal of Microwave Power and Electromagnetic Energy 27 (1992) 11–22.
[8] Deepak, J.W. Evans, Calculation of temperatures in microwave-heated two-dimensional ceramic bodies, Journal of American Ceramic Society 76 (1993) 1915–1923.
[9] F. Liu, I. Turner, M. Bialkowski, A finite-difference time-domain simulation of power density distribution in a dielectric loaded microwave cavity, Journal of Microwave Power and Electromagnetic Energy 29 (1994) 138–147.
[10] K. Iwabuchi, T. Kubota, T. Kashiwa, H. Tagashira, Analysis of electromagnetic fields using the finite-difference time-domain method in a microwave oven loaded with high-loss dielectric, Electronics and Communications in Japan 78 (1997) 41–50.
[11] D.C. Dibben, A.C. Metaxas, Frequency domain vs. time domain finite element methods for calculation of fields in multimode cavities, IEEE Transaction on Magnetics 33 (1997) 1468–1471.
[12] D.C. Dibben, A.C. Metaxas, Finite element time domain analysis of multimode applicators using edge elements, Journal of Microwave Power and Electromagnetic Energy 29 (1994) 243–251.
[13] G.A. Kriegsmann, Cavity effects in microwave heating of ceramics, Journal of Applied Mathematics 57 (1997) 382–400.
[14] J.C. Araneta, M.E. Brodwin, G.A. Kriegsmann, High-temperature microwave characterization of dielectric rods, IEEE Transactions on Microwave Theory and Techniques 32 (1984) 1328–1335.
[15] K.S. Yee, Numerical solution of initial boundary value problem involving Maxwell's equations in isotropic media, IEEE Transactions on Antennas and Propagation 14 (1966) 302–307.
[16] J.P. Webb, G.L. Maile, R.L. Ferrari, Finite element implementation of three dimensional electromagnetic problems, IEEE Proceedings 78 (1983) 196–200.
[17] H. Zhao, I.W. Turner, An analysis of the finite-difference time-domain method for modeling the microwave heating of dielectric materials within a three-dimensional cavity system, Journal of Microwave Power and Electromagnetic Energy 31 (1996) 199–214.
[18] H. Zhang, A.K. Taub, I.A. Doona, Electromagnetics, heat transfer and thermokinetics in microwave sterilization, AIChE Journal 47 (2001) 1957–1968.
[19] K.G. Ayappa, H.T. Davis, E.A. Davis, J. Gordon, Two-dimensional finite element analysis of microwave heating, AIChE Journal 38 (1992) 1577–1592.
[20] K.G. Ayappa, S. Brandon, J.J. Derby, H.T. Davis, E.A. Davis, Microwave driven convection in a square cavity, AIChE Journal 40 (1994) 1268–1272.
[21] K.G. Ayappa, T. Sengupta, Microwave heating in multiphase systems: evaluation of series solutions, Journal of Engineering Mathematics 44 (2002) 155–171.
[22] T. Basak, K.G. Ayappa, Analysis of microwave thawing of slabs with effective heat capacity method, AIChE Journal 43 (1997) 1662–1667.
[23] P. Ratanadecho, K. Aoki, M. Akahori, The characteristics of microwave melting of frozen packed beds using a rectangular waveguide, IEEE Transactions on Microwave Theory and Techniques 50 (2002) 1495–1502.
[24] P. Ratanadecho, K. Aoki, M. Akahori, Influence of irradiation time, particle sizes, and initial moisture content during microwave drying of multilayered capillary porous materials, Journal of Heat Transfer 124 (2002) 151–161.
[25] A. Datta, H. Prosetya, W. Hu, Mathematical modeling of batch heating of liquids in a microwave cavity, Journal of Microwave Power and Electromagnetic Energy 27 (1992) 38–48.
[26] P. Ratanadecho, K. Aoki, M. Akahori, A numerical and experimental investigation of the modeling of microwave heating for liquid layers using a rectangular wave guide (effects of natural convection and dielectric properties), Applied Mathematical Modeling 26 (2002) 449–472.
[27] J. Zhu, A.V. Kuznetsov, K.P. Sandeep, Numerical simulation of forced convection in a duct subjected to microwave heating, Heat and Mass Transfer, http://dx.doi.org/10.1007/s00231-006-0105-y (online first).
[28] T. Basak, K.G. Ayappa, Role of length scales on microwave thawing dynamics in 2D cylinders, International Journal of Heat and Mass Transfer 45 (2002) 4543–4559.
[29] K.G. Ayappa, H.T. Davis, S.A. Barringer, E.A. Davis, Resonant microwave power absorption in slabs and cylinders, AIChE Journal 43 (1997) 615–624.
[30] D.K. Cheng, Field and Wave Electromagnetics, Addison-Wesley, New York, 1992.
[31] G. Mur, Absorbing boundary conditions for the finite difference approximation of the time domain electromagnetic field equations, IEEE Transactions on Electromagnetic Compatibility 23 (1981) 377–382.
[32] Q. Zhang, Numerical simulation of heating of a containerized liquid in a single-mode microwave cavity, MS thesis, Indiana University–Purdue University at Indianapolis, IN, 1998.
[33] R.B. Bird, W.E. Stewart, E.N. Lightfoot, Transport Phenomena, John Wiley & Sons, New York, 2002.
[34] K.S. Kunz, R. Luebbers, The Finite Difference Time Domain Method for Electromagnetics, CRC, Boca Raton, FL, 1993.
[35] S. Dey, R. Mittra, A conformal finite-difference time-domain technique for modeling cylindrical dielectric resonators, IEEE Transactions on Microwave Theory and Techniques 47 (1999) 1737–1739.
[36] Yu.V. Bykov, K.I. Rybakov, V.E. Semenov, High-temperature microwave processing of materials, Journal of Physics D: Applied Physics 34 (2001) 55–75.